

Supporting Material for:

Capsaicin Interaction with TRPV1 Channels in a Lipid Bilayer: Molecular Dynamics Simulation

Sonya M. Hanson, Simon Newstead, Kenton J. Swartz, & Mark S.P. Sansom

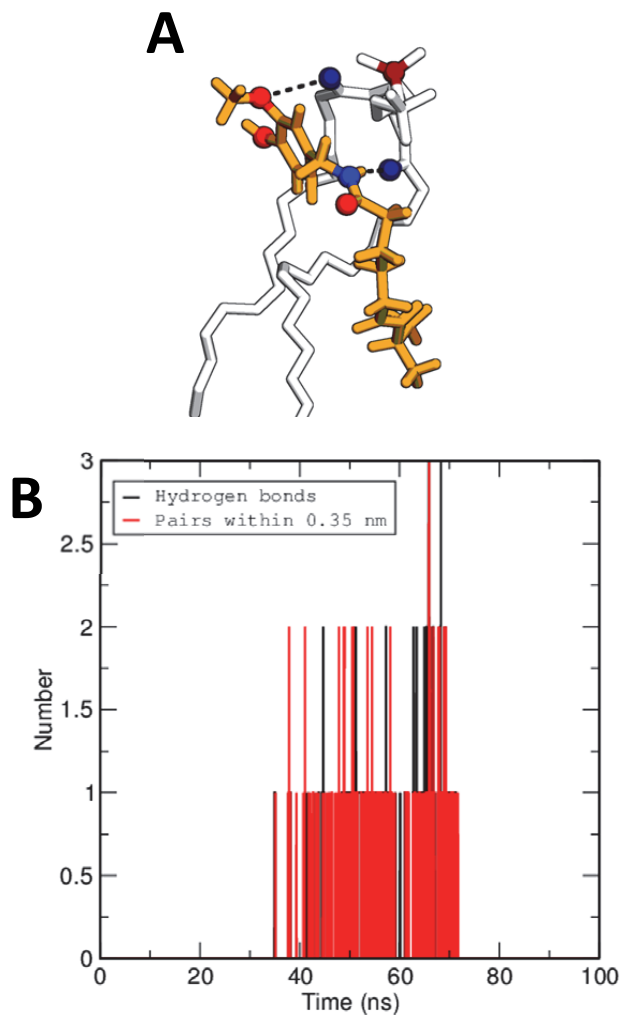


FIGURE S1 POPC and Capsaicin hydrogen bonding interaction. (A) An example of a long-lived hydrogen bonding interaction between a carbonyl group of a POPC molecule (in white) and the B region of capsaicin (in orange). (B) Number of H-bonds vs. time between capsaicin and the selected POPC molecule. This interaction is maintained for more than 30 ns of the simulation.

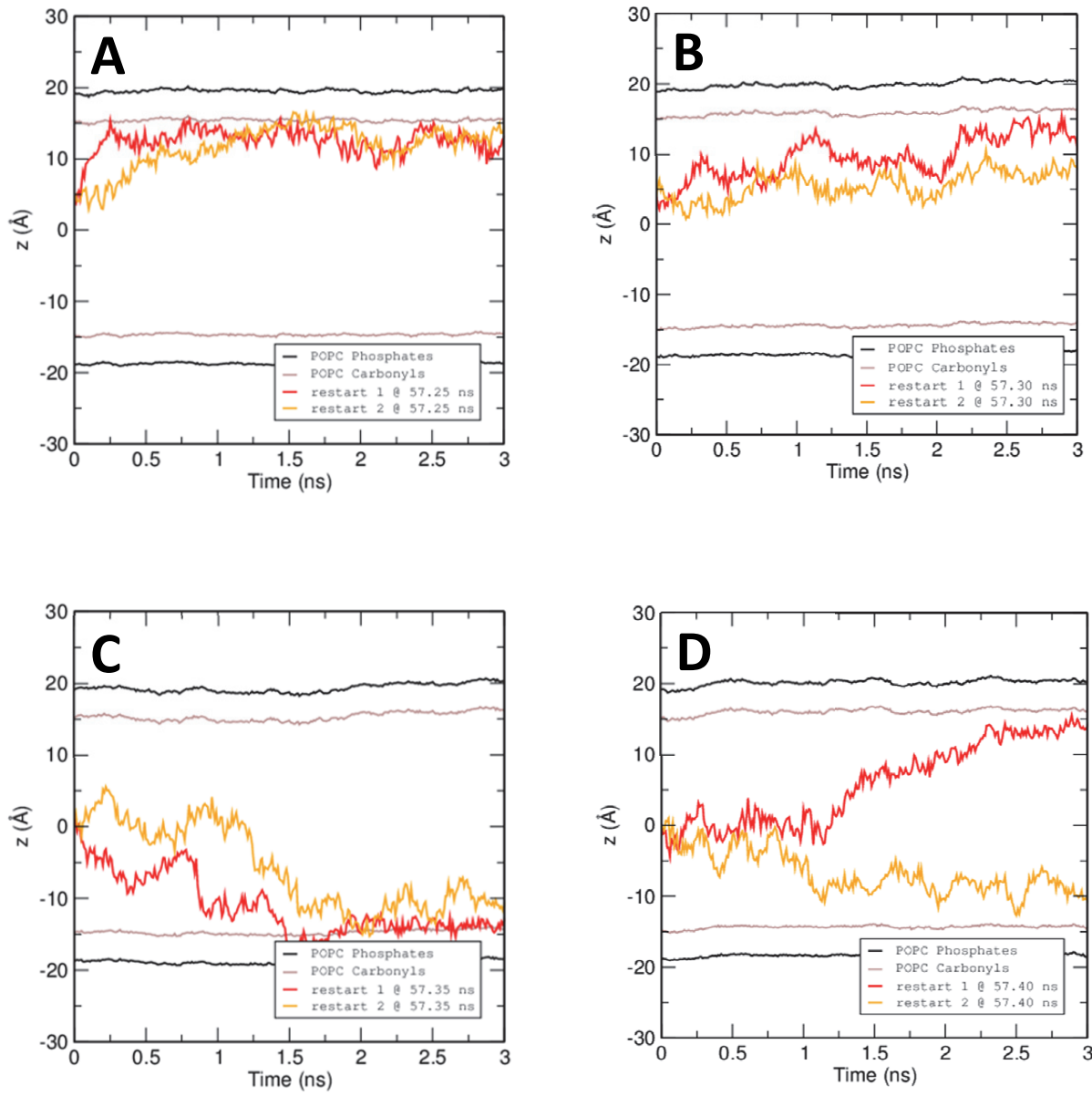


FIGURE S2 Multiple simulations initiated at selected points along the original capsaicin flip-flop trajectory. (A) Shows two repeats (red and orange lines) with different random velocity seeds using a starting position at 57.25 ns, (B) at 57.30 ns, (C) at 57.35 ns, and (D) at 57.40 ns along the original trajectory which yielded a flip-flop event. Red or orange lines represent the center of mass of capsaicin during different repeats. Black lines represent the phosphate head groups of POPC. Brown lines represent the carbonyls of POPC.

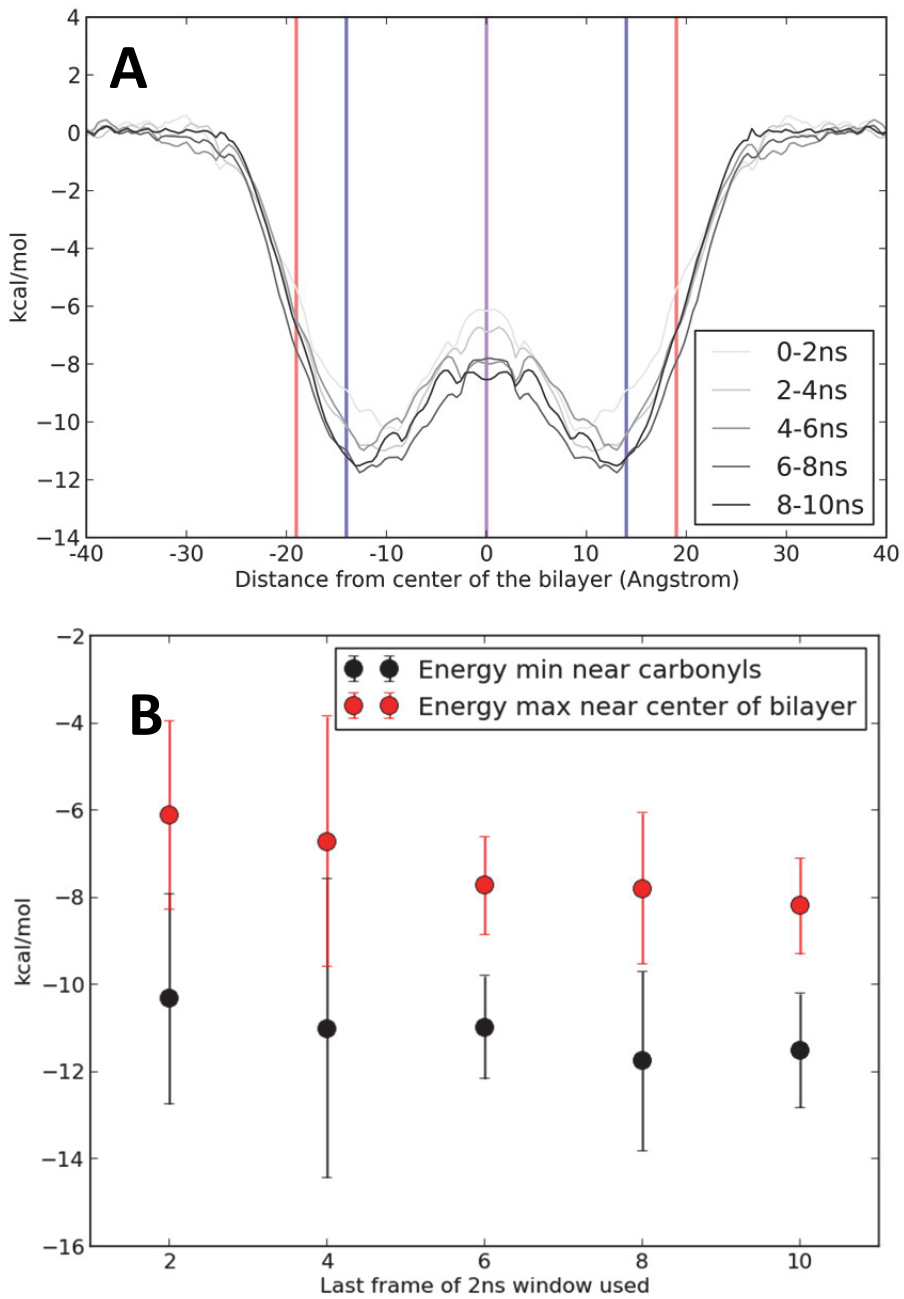


FIGURE S3 PMF Convergence. (A) PMF profiles as calculated from consecutive 2 ns segments of the full 10 ns simulations of 1 Å windows across the bilayer. (B) The values of the energy minima near the carbonyls ($z = \pm 12 \text{ \AA}$) and the energy maxima near the center of the bilayer ($z = 0 \text{ \AA}$) were calculated for the consecutive PMFs in A to provide a measure of convergence of the free energy profile.

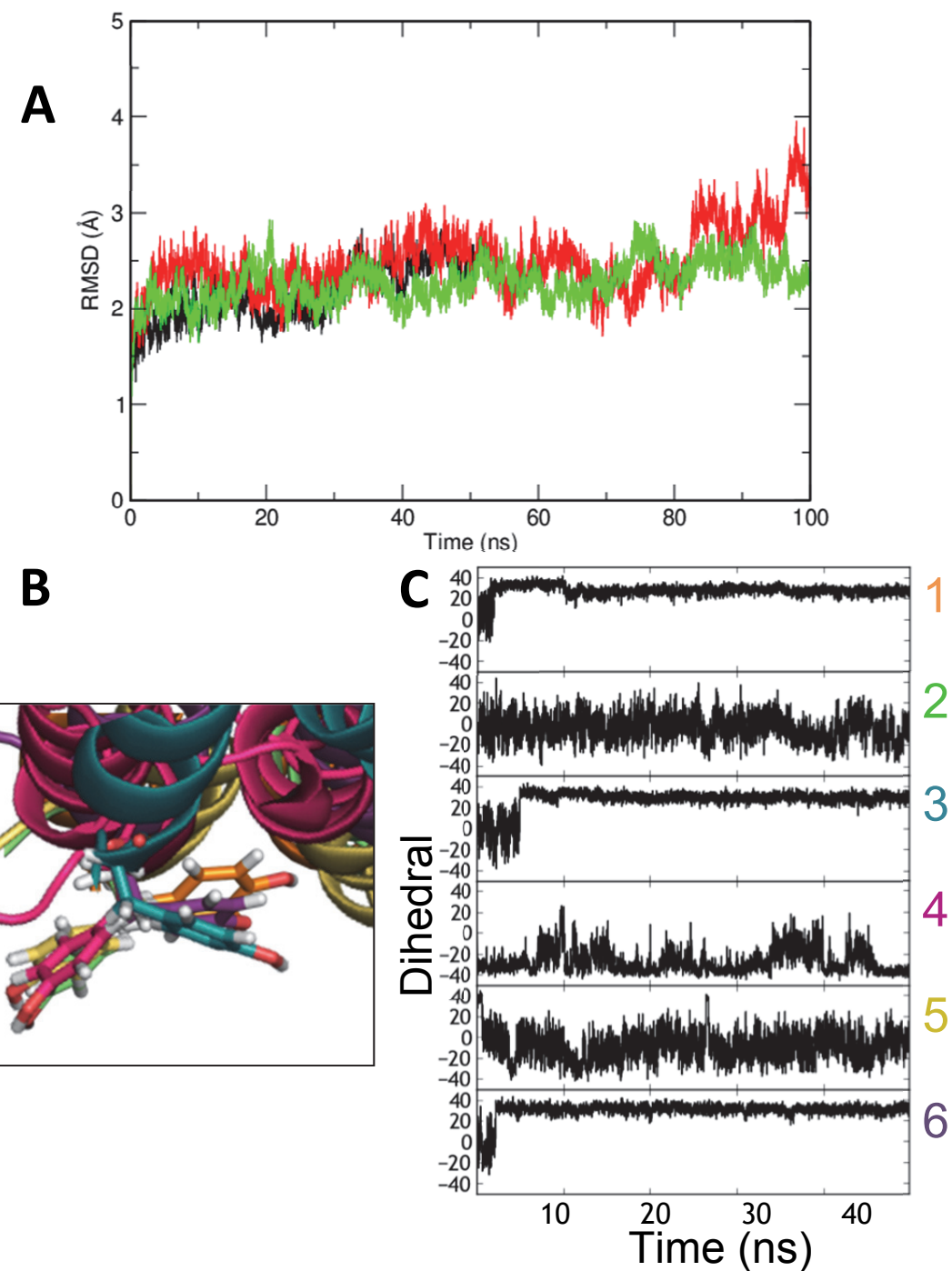


FIGURE S4 Analysis of stability of the TRPV1 S1-S4 in model membrane. (A) The backbone RMSD from the initial structure of the S1-S4 domain of TRPV1 over the course of three repeat 100 ns simulations. (B) The flip from an outward to an inward conformation of the sidechain of tyrosine 511. (C) Changes in the X_1 dihedral angle of Tyr511 over time of six separate simulations (colored accordingly) of the S1-S4 of the apo EM structure in a POPC bilayer.

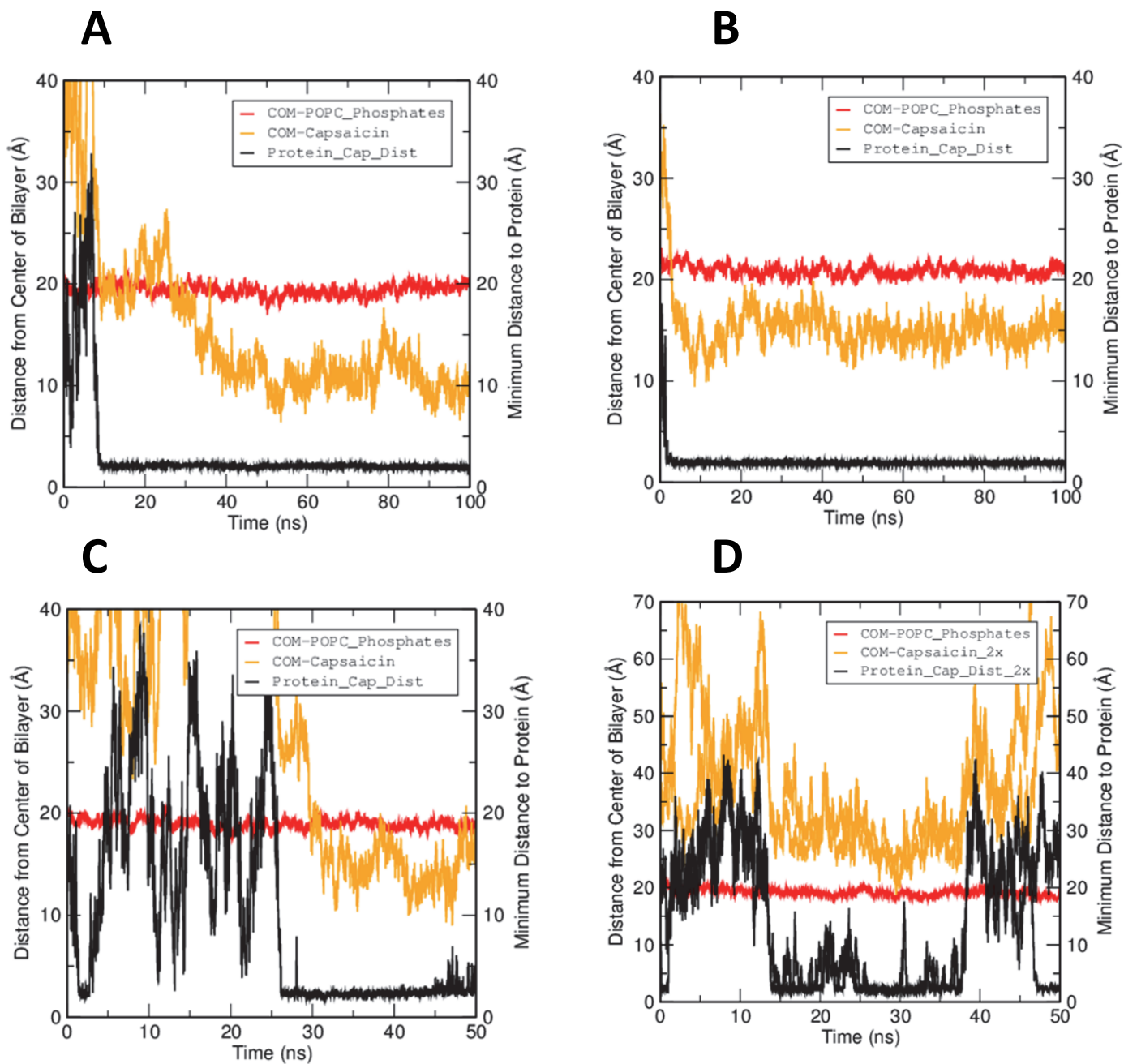


FIGURE S5 Capsaicin interaction with TRPV1 S1-S4 compared to its membrane penetration. Plots of the minimum distance of interacting capsaicin molecules to the TRPV1 S1-S4 domain over the course of four simulations (black), overlaid with the bilayer penetration as shown by the center of mass of capsaicin (orange) relative to that of the phosphates of the intracellular leaflet (red). This is shown for two capsaicin molecules that interact with the S1 helix (A) and (B), and for three capsaicin molecules that interact with the S2-S3 loop (C) and (D). (D) is an interaction between a two-capsaicin aggregate and the TRPV1 S1-S4. Notice how in A-C the capsaicin interacts with the protein before and during bilayer penetration.

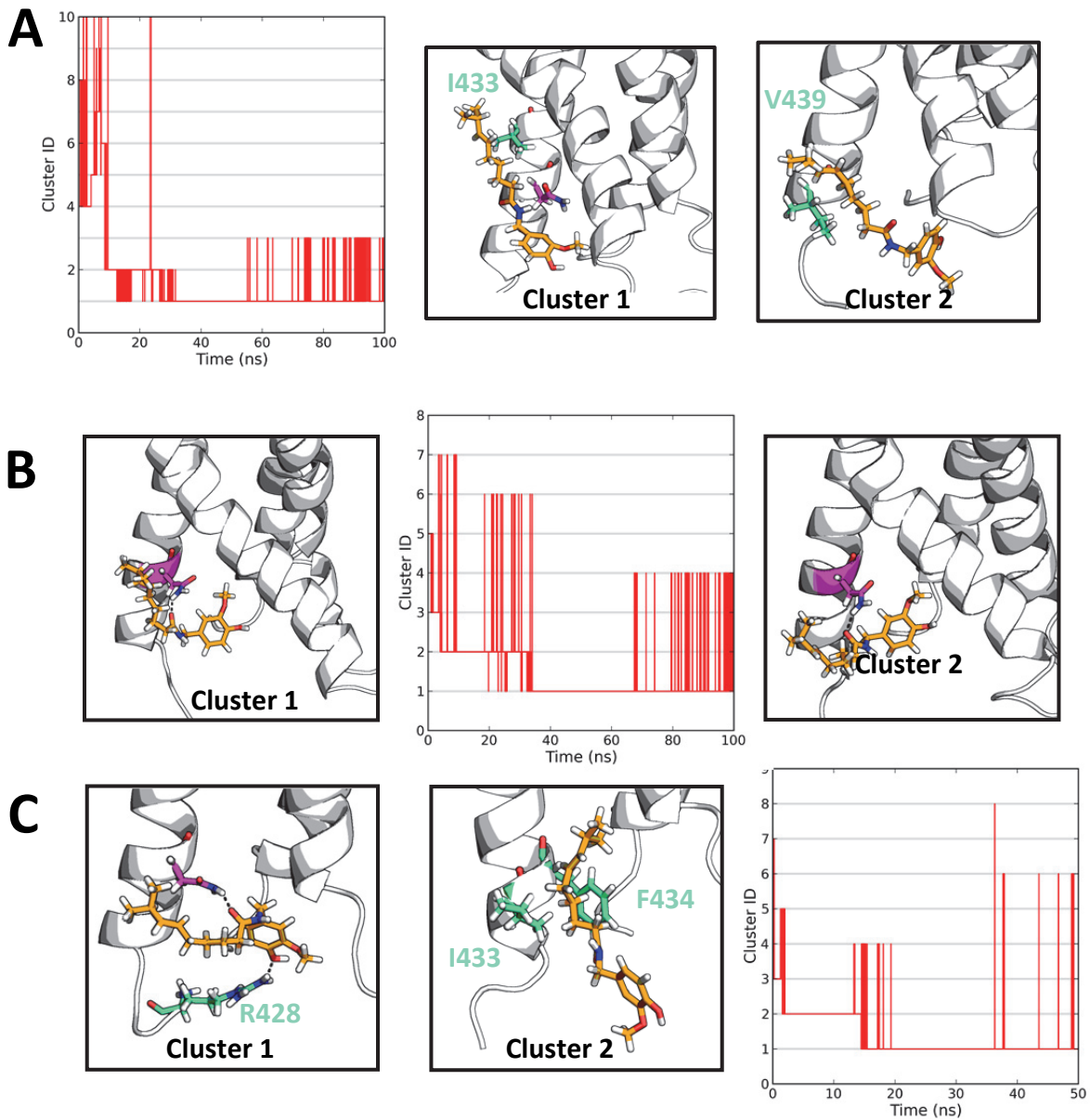


FIGURE S6 Results of cluster analysis for ‘encounter complex’ simulations in which interactions are seen between capsaicin and the S1 helix. (A) Cluster analysis of one 100 ns simulation results in a final cluster that involves N437 (magenta), but also I433 (teal). In the second-most dominant cluster the interaction with N437 is not seen, and V439 (teal) instead is seen to interact with capsaicin, perhaps on its way to a more stable pose. (B) This 100 ns simulation is also the one shown in Fig. 7. Cluster analysis shows a dominant cluster in which capsaicin interacts with N437 (magenta). The second-most dominant cluster also shares this interaction, but the C group acyl chain tail is in a different orientation. (C) In this 50 ns simulation, an interaction between capsaicin and the S1 helix is also seen, and the N437 (magenta) interaction is once again observed in the most dominant cluster. However, the R428 (teal) interaction is also seen. This interaction may be an artifact of the S1-S4 helices being truncated from the rest of the full length protein, although it is not seen in the other two simulations.

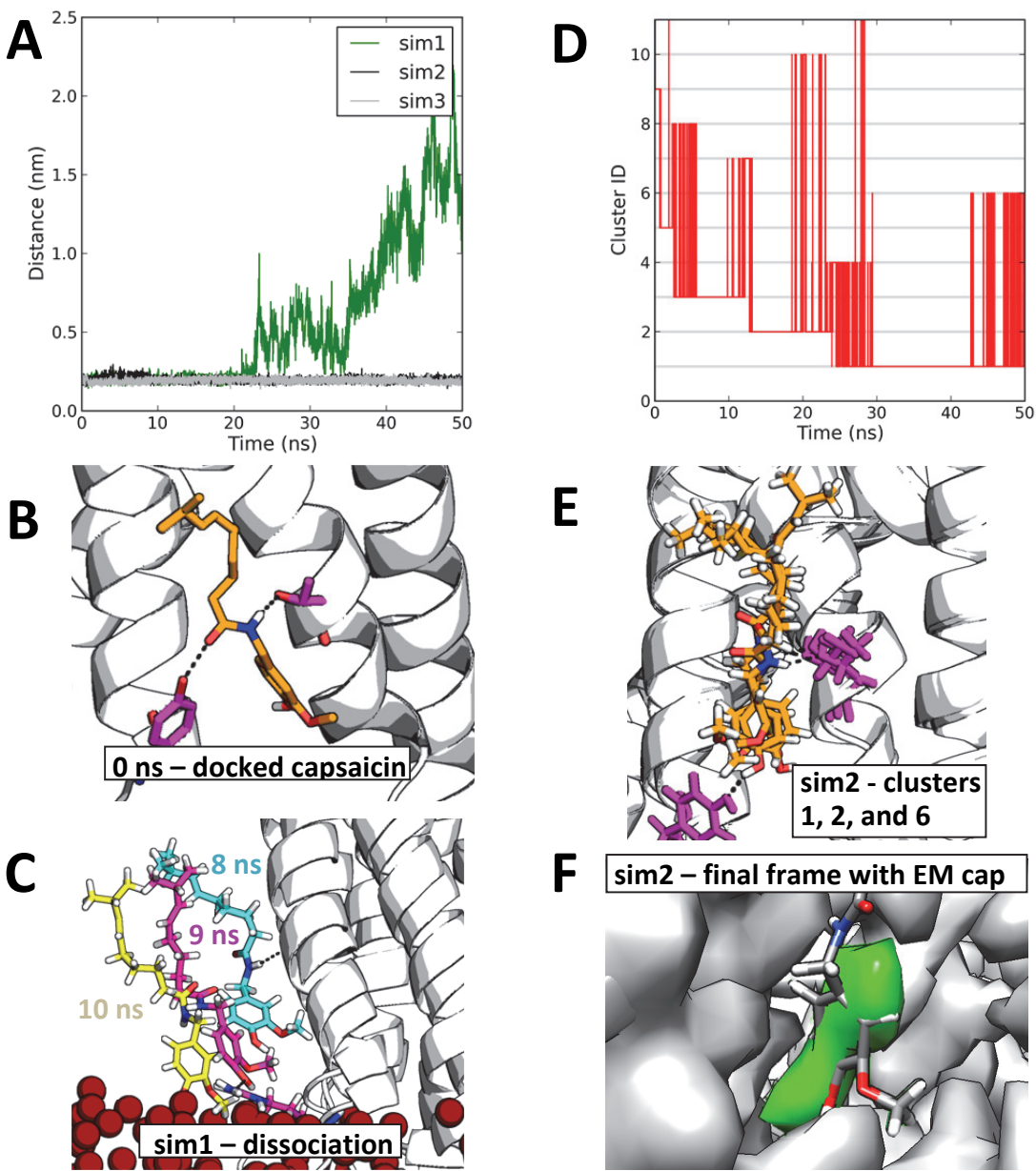


FIGURE S7 Results of 50ns simulation of capsaicin docked to TRPV1. (A) In two out of three simulations capsaicin continued to equilibrate within the docked position between the S3 and S4. (B) The docked pose of capsaicin was the top-ranked pose found using the Autodock Vina program and the full-length TRPV1 (PDB ID: 3J5R). T550 and Y511 are shown in magenta. (C) In the simulation in which capsaicin dissociated from the S1-S4 helices it initially had formed a hydrogen bond with T550 (cyan) and then began to dissociate, interacting with an arginine at the intracellular side of the S4 (magenta) and then finally with only the POPC molecules (yellow) in a position seen in the capsaicin-bilayer only simulations. (D) Cluster analysis of one of the simulations in which capsaicin remained in the docked pose shows small shifts toward a final cluster. (E) Three of the dominant clusters from D (1, 2, and 6) are shown. A change from the initial docked pose is that now Y511 forms a hydrogen bonding interaction with the A group aromatic region instead of the B group. (F) An overlay of the final frame of this simulation shows that the A group of capsaicin overlaps with density suspected to correspond to capsaicin in the sharpened EM density (deep green) of the capsaicin bound structure (temperature factor -200 Å, filtered to 4.2 Å, shown at sigma level 8).

Supporting Material - Parameter (*.itp) file for capsaicin

```

[ moleculetype ]
; name nrexcl
CAP 3

[ atoms ]
; nr type resnr residu atom cgnr charge mass
  1 opls_145 1 CAP C1 1 -0.11500 12.01100 ; -0.1150000
  2 opls_146 1 CAP H12 1 0.11500 1.00800 ; 0.0000000
  3 opls_145 1 CAP C2 2 -0.11500 12.01100 ; -0.1150000
  4 opls_145 1 CAP C3 3 -0.11500 12.01100 ; -0.2300000
  5 opls_146 1 CAP H13 3 0.11500 1.00800 ; -0.1150000
  6 opls_145 1 CAP C4 4 -0.11500 12.01100 ; -0.2300000
  7 opls_146 1 CAP H14 4 0.11500 1.00800 ; -0.1150000
  8 opls_166 1 CAP C5 5 0.15000 12.01100 ; 0.0350000
  9 opls_166 1 CAP C6 6 0.15000 12.01100 ; 0.1850000
 10 opls_179 1 CAP O1 6 -0.28500 15.99940 ; -0.1000000
 11 opls_157 1 CAP C7 7 0.13000 12.01100 ; 0.0450000
 12 opls_156 1 CAP H17 7 0.04000 1.00800 ; 0.0850000
 13 opls_156 1 CAP H18 7 0.04000 1.00800 ; 0.1250000
 14 opls_156 1 CAP H19 7 0.04000 1.00800 ; 0.1650000
 15 opls_167 1 CAP O2 5 -0.58500 15.99940 ; -0.4200000
 16 opls_168 1 CAP H20 5 0.43500 1.00800 ; 0.0150000
 17 opls_244 1 CAP C8 8 0.08000 12.01100 ; 0.0950000
 18 opls_140 1 CAP H10 8 0.06000 1.00800 ; 0.1550000
 19 opls_140 1 CAP H11 8 0.06000 1.00800 ; 0.2150000
 20 opls_238 1 CAP N1 8 -0.50000 14.00670 ; -0.2850000
 21 opls_241 1 CAP H21 8 0.30000 1.00800 ; 0.0150000
 22 opls_235 1 CAP C9 9 0.50000 12.01100 ; 0.5150000
 23 opls_136 1 CAP C10 10 -0.12000 12.01100 ; 0.3950000
 24 opls_140 1 CAP H8 10 0.06000 1.00800 ; 0.4550000
 25 opls_140 1 CAP H9 10 0.06000 1.00800 ; 0.5150000
 26 opls_236 1 CAP O3 9 -0.50000 15.99940 ; 0.0150000
 27 opls_136 1 CAP C11 11 -0.12000 12.01100 ; -0.1050000
 28 opls_140 1 CAP H7 11 0.06000 1.00800 ; -0.0450000
 29 opls_140 1 CAP H16 11 0.06000 1.00800 ; 0.0150000
 30 opls_136 1 CAP C12 12 -0.12000 12.01100 ; -0.1050000
 31 opls_140 1 CAP H5 12 0.06000 1.00800 ; -0.0450000
 32 opls_140 1 CAP H6 12 0.06000 1.00800 ; 0.0150000
 33 opls_136 1 CAP C13 13 -0.12000 12.01100 ; -0.1050000
 34 opls_140 1 CAP H4 13 0.06000 1.00800 ; -0.0450000
 35 opls_140 1 CAP H15 13 0.06000 1.00800 ; 0.0150000
 36 opls_142 1 CAP C14 14 -0.11500 12.01100 ; -0.1000000
 37 opls_144 1 CAP H3 14 0.11500 1.00800 ; 0.0150000
 38 opls_142 1 CAP C15 15 -0.11500 12.01100 ; -0.1000000
 39 opls_144 1 CAP H1 15 0.11500 1.00800 ; 0.0150000
 40 opls_137 1 CAP C16 16 -0.06000 12.01100 ; -0.0450000
 41 opls_140 1 CAP H2 16 0.06000 1.00800 ; 0.0150000
 42 opls_135 1 CAP C17 17 -0.18000 12.01100 ; -0.1650000
 43 opls_140 1 CAP H25 17 0.06000 1.00800 ; -0.1050000
 44 opls_140 1 CAP H26 17 0.06000 1.00800 ; -0.0450000
 45 opls_140 1 CAP H27 17 0.06000 1.00800 ; 0.0150000
 46 opls_135 1 CAP C18 18 -0.18000 12.01100 ; -0.1650000
 47 opls_140 1 CAP H22 18 0.06000 1.00800 ; -0.1050000
 48 opls_140 1 CAP H23 18 0.06000 1.00800 ; -0.0450000
 49 opls_140 1 CAP H24 18 0.06000 1.00800 ; 0.0150000
; total molecule charge = 0.0000000

```

```

[ bonds ]
; ai aj funct b0 kb
  1   3   1  0.14000 392459. ; C1- C2
  1   9   1  0.14000 392459. ; C1- C6
  3   4   1  0.14000 392459. ; C2- C3

```

4	6	1	0.14000	392459.	;	C3-	C4
6	8	1	0.14000	392459.	;	C4-	C5
8	9	1	0.14000	392459.	;	C5-	C6
9	10	1	0.13640	376560.	;	C6-	O1
10	11	1	0.14100	267776.	;	O1-	C7
8	15	1	0.13640	376560.	;	C5-	O2
3	17	1	0.15100	265266.	;	C2-	C8
17	20	1	0.14490	282002.	;	C8-	N1
20	22	1	0.13350	410032.	;	N1-	C9
22	23	1	0.15220	265266.	;	C9-	C10
22	26	1	0.12290	476976.	;	C9-	O3
23	27	1	0.15290	224262.	;	C10-	C11
27	30	1	0.15290	224262.	;	C11-	C12
30	33	1	0.15290	224262.	;	C12-	C13
33	36	1	0.15100	265266.	;	C13-	C14
36	38	1	0.13400	459403.	;	C14-	C15
38	40	1	0.15100	265266.	;	C15-	C16
40	42	1	0.15290	224262.	;	C16-	C17
40	46	1	0.15290	224262.	;	C16-	C18
38	39	1	0.10800	307106.	;	C15-	H1
40	41	1	0.10900	284512.	;	C16-	H2
36	37	1	0.10800	307106.	;	C14-	H3
33	34	1	0.10900	284512.	;	C13-	H4
30	31	1	0.10900	284512.	;	C12-	H5
30	32	1	0.10900	284512.	;	C12-	H6
27	28	1	0.10900	284512.	;	C11-	H7
23	24	1	0.10900	284512.	;	C10-	H8
23	25	1	0.10900	284512.	;	C10-	H9
17	18	1	0.10900	284512.	;	C8-	H10
17	19	1	0.10900	284512.	;	C8-	H11
1	2	1	0.10800	307106.	;	C1-	H12
4	5	1	0.10800	307106.	;	C3-	H13
6	7	1	0.10800	307106.	;	C4-	H14
33	35	1	0.10900	284512.	;	C13-	H15
27	29	1	0.10900	284512.	;	C11-	H16
11	12	1	0.10900	284512.	;	C7-	H17
11	13	1	0.10900	284512.	;	C7-	H18
11	14	1	0.10900	284512.	;	C7-	H19
15	16	1	0.09450	462750.	;	O2-	H20
20	21	1	0.10100	363171.	;	N1-	H21
46	47	1	0.10900	284512.	;	C18-	H22
46	48	1	0.10900	284512.	;	C18-	H23
46	49	1	0.10900	284512.	;	C18-	H24
42	43	1	0.10900	284512.	;	C17-	H25
42	44	1	0.10900	284512.	;	C17-	H26
42	45	1	0.10900	284512.	;	C17-	H27

[constraints]
 8 16 2 0.19393 ; C5 H20

[pairs]
 9 4 1 ; C6- C3
 9 17 1 ; C6- C8
 2 4 1 ; H12- C3
 2 17 1 ; H12- C8
 3 8 1 ; C2- C5
 3 10 1 ; C2- O1
 2 8 1 ; H12- C5
 2 10 1 ; H12- O1
 1 6 1 ; C1- C4
 1 5 1 ; C1- H13
 17 6 1 ; C8- C4
 17 5 1 ; C8- H13
 3 7 1 ; C2- H14

5	8	1	;	H13-	C5
5	7	1	;	H13-	H14
4	15	1	;	C3-	O2
7	9	1	;	H14-	C6
7	15	1	;	H14-	O2
6	10	1	;	C4-	O1
15	1	1	;	O2-	C1
15	10	1	;	O2-	O1
1	11	1	;	C1-	C7
8	11	1	;	C5-	C7
9	12	1	;	C6-	H17
9	13	1	;	C6-	H18
9	14	1	;	C6-	H19
6	16	1	;	C4-	H20
9	16	1	;	C6-	H20
1	20	1	;	C1-	N1
1	18	1	;	C1-	H10
1	19	1	;	C1-	H11
4	20	1	;	C3-	N1
4	18	1	;	C3-	H10
4	19	1	;	C3-	H11
3	22	1	;	C2-	C9
3	21	1	;	C2-	H21
18	22	1	;	H10-	C9
18	21	1	;	H10-	H21
19	22	1	;	H11-	C9
19	21	1	;	H11-	H21
17	23	1	;	C8-	C10
17	26	1	;	C8-	O3
21	23	1	;	H21-	C10
21	26	1	;	H21-	O3
20	27	1	;	N1-	C11
20	24	1	;	N1-	H8
20	25	1	;	N1-	H9
26	27	1	;	O3-	C11
26	24	1	;	O3-	H8
26	25	1	;	O3-	H9
22	30	1	;	C9-	C12
22	28	1	;	C9-	H7
22	29	1	;	C9-	H16
24	30	1	;	H8-	C12
24	28	1	;	H8-	H7
24	29	1	;	H8-	H16
25	30	1	;	H9-	C12
25	28	1	;	H9-	H7
25	29	1	;	H9-	H16
23	33	1	;	C10-	C13
23	31	1	;	C10-	H5
23	32	1	;	C10-	H6
28	33	1	;	H7-	C13
28	31	1	;	H7-	H5
28	32	1	;	H7-	H6
29	33	1	;	H16-	C13
29	31	1	;	H16-	H5
29	32	1	;	H16-	H6
27	36	1	;	C11-	C14
27	34	1	;	C11-	H4
27	35	1	;	C11-	H15
31	36	1	;	H5-	C14
31	34	1	;	H5-	H4
31	35	1	;	H5-	H15
32	36	1	;	H6-	C14
32	34	1	;	H6-	H4
32	35	1	;	H6-	H15
30	38	1	;	C12-	C15

30	37	1	;	C12-	H3
34	38	1	;	H4-	C15
34	37	1	;	H4-	H3
35	38	1	;	H15-	C15
35	37	1	;	H15-	H3
33	40	1	;	C13-	C16
33	39	1	;	C13-	H1
37	40	1	;	H3-	C16
37	39	1	;	H3-	H1
36	42	1	;	C14-	C17
36	46	1	;	C14-	C18
36	41	1	;	C14-	H2
39	42	1	;	H1-	C17
39	46	1	;	H1-	C18
39	41	1	;	H1-	H2
38	43	1	;	C15-	H25
38	44	1	;	C15-	H26
38	45	1	;	C15-	H27
46	43	1	;	C18-	H25
46	44	1	;	C18-	H26
46	45	1	;	C18-	H27
41	43	1	;	H2-	H25
41	44	1	;	H2-	H26
41	45	1	;	H2-	H27
38	47	1	;	C15-	H22
38	48	1	;	C15-	H23
38	49	1	;	C15-	H24
42	47	1	;	C17-	H22
42	48	1	;	C17-	H23
42	49	1	;	C17-	H24
41	47	1	;	H2-	H22
41	48	1	;	H2-	H23
41	49	1	;	H2-	H24

[angles]							
;	ai	aj	ak	funct	th0	cth	
	9	1	3	1	120.000	527.1840	;
	2	1	3	1	120.000	292.8800	;
	1	3	4	1	120.000	527.1840	;
	1	3	17	1	120.000	585.7600	;
	2	1	9	1	120.000	292.8800	;
	1	9	8	1	120.000	527.1840	;
	1	9	10	1	120.000	585.7600	;
	17	3	4	1	120.000	585.7600	;
	3	4	6	1	120.000	527.1840	;
	3	4	5	1	120.000	292.8800	;
	5	4	6	1	120.000	292.8800	;
	4	6	8	1	120.000	527.1840	;
	4	6	7	1	120.000	292.8800	;
	7	6	8	1	120.000	292.8800	;
	6	8	9	1	120.000	527.1840	;
	6	8	15	1	120.000	585.7600	;
	15	8	9	1	120.000	585.7600	;
	8	9	10	1	120.000	585.7600	;
	9	10	11	1	111.000	627.6000	;
	10	11	12	1	109.500	292.8800	;
	10	11	13	1	109.500	292.8800	;
	10	11	14	1	109.500	292.8800	;
	8	15	16	1	113.000	292.8800	;
	3	17	20	1	109.700	669.4400	;
	3	17	18	1	109.500	292.8800	;
	3	17	19	1	109.500	292.8800	;
	18	17	20	1	109.500	292.8800	;
	19	17	20	1	109.500	292.8800	;
	17	20	22	1	121.900	418.4000	;
							N1-
							C9

17	20	21	1	118.400	317.9840	;	C8-	N1-	H21
21	20	22	1	119.800	292.8800	;	H21-	N1-	C9
20	22	23	1	116.600	585.7600	;	N1-	C9-	C10
20	22	26	1	122.900	669.4400	;	N1-	C9-	O3
26	22	23	1	120.400	669.4400	;	O3-	C9-	C10
22	23	27	1	111.100	527.1840	;	C9-	C10-	C11
22	23	24	1	109.500	292.8800	;	C9-	C10-	H8
22	23	25	1	109.500	292.8800	;	C9-	C10-	H9
24	23	27	1	110.700	313.8000	;	H8-	C10-	C11
25	23	27	1	110.700	313.8000	;	H9-	C10-	C11
23	27	30	1	112.700	488.2730	;	C10-	C11-	C12
23	27	28	1	110.700	313.8000	;	C10-	C11-	H7
23	27	29	1	110.700	313.8000	;	C10-	C11-	H16
28	27	30	1	110.700	313.8000	;	H7-	C11-	C12
29	27	30	1	110.700	313.8000	;	H16-	C11-	C12
27	30	33	1	112.700	488.2730	;	C11-	C12-	C13
27	30	31	1	110.700	313.8000	;	C11-	C12-	H5
27	30	32	1	110.700	313.8000	;	C11-	C12-	H6
31	30	33	1	110.700	313.8000	;	H5-	C12-	C13
32	30	33	1	110.700	313.8000	;	H6-	C12-	C13
30	33	36	1	111.100	527.1840	;	C12-	C13-	C14
30	33	34	1	110.700	313.8000	;	C12-	C13-	H4
30	33	35	1	110.700	313.8000	;	C12-	C13-	H15
34	33	36	1	109.500	292.8800	;	H4-	C13-	C14
35	33	36	1	109.500	292.8800	;	H15-	C13-	C14
33	36	38	1	124.000	585.7600	;	C13-	C14-	C15
33	36	37	1	117.000	292.8800	;	filled		
37	36	38	1	120.000	292.8800	;	H3-	C14-	C15
36	38	40	1	124.000	585.7600	;	C14-	C15-	C16
36	38	39	1	120.000	292.8800	;	C14-	C15-	H1
39	38	40	1	117.000	292.8800	;	filled		
38	40	42	1	111.100	527.1840	;	C15-	C16-	C17
38	40	46	1	111.100	527.1840	;	C15-	C16-	C18
38	40	41	1	109.500	292.8800	;	C15-	C16-	H2
46	40	42	1	112.700	488.2730	;	C18-	C16-	C17
41	40	42	1	110.700	313.8000	;	H2-	C16-	C17
40	42	43	1	110.700	313.8000	;	C16-	C17-	H25
40	42	44	1	110.700	313.8000	;	C16-	C17-	H26
40	42	45	1	110.700	313.8000	;	C16-	C17-	H27
41	40	46	1	110.700	313.8000	;	H2-	C16-	C18
40	46	47	1	110.700	313.8000	;	C16-	C18-	H22
40	46	48	1	110.700	313.8000	;	C16-	C18-	H23
40	46	49	1	110.700	313.8000	;	C16-	C18-	H24
35	33	34	1	107.800	276.1440	;	H15-	C13-	H4
32	30	31	1	107.800	276.1440	;	H6-	C12-	H5
29	27	28	1	107.800	276.1440	;	H16-	C11-	H7
25	23	24	1	107.800	276.1440	;	H9-	C10-	H8
19	17	18	1	107.800	276.1440	;	H11-	C8-	H10
13	11	12	1	107.800	276.1440	;	H18-	C7-	H17
14	11	12	1	107.800	276.1440	;	H19-	C7-	H17
14	11	13	1	107.800	276.1440	;	H19-	C7-	H18
48	46	47	1	107.800	276.1440	;	H23-	C18-	H22
49	46	47	1	107.800	276.1440	;	H24-	C18-	H22
49	46	48	1	107.800	276.1440	;	H24-	C18-	H23
44	42	43	1	107.800	276.1440	;	H26-	C17-	H25
45	42	43	1	107.800	276.1440	;	H27-	C17-	H25
45	42	44	1	107.800	276.1440	;	H27-	C17-	H26

```

[ dihedrals ]
; ai aj ak al funct c0 c1 c2 c3 c4 c5
; 9 1 3 4 3 30.33400 0.00000 -30.33400 0.00000 0.00000 ; dih
3 1 9 8 3 30.33400 0.00000 -30.33400 0.00000 0.00000 ; dih
1 3 4 6 3 30.33400 0.00000 -30.33400 0.00000 0.00000 ; dih
3 4 6 8 3 30.33400 0.00000 -30.33400 0.00000 0.00000 ; dih
4 6 8 9 3 30.33400 0.00000 -30.33400 0.00000 0.00000 ; dih
6 8 9 1 3 30.33400 0.00000 -30.33400 0.00000 0.00000 ; dih
1 9 10 11 3 12.55200 0.00000 -12.55200 0.00000 0.00000 ; dih
9 10 11 12 3 1.589992 4.76976 0.00000 -6.35968 0.00000 ; dih
6 8 15 16 3 7.03749 0.00000 -7.03749 0.00000 0.00000 ; dih
1 3 17 20 3 0.00000 0.00000 0.00000 0.00000 0.00000 ; dih
17 20 22 23 3 30.28798 -4.81160 -25.47638 0.00000 0.00000 ; dih
20 22 23 27 3 4.83252 -7.65254 1.68196 1.13805 0.00000 ; dih
1 3 27 30 3 -4.96013 6.28646 1.30959 -2.63592 0.00000 ; dih
22 23 27 33 3 2.92880 -1.46440 0.20920 -1.67360 0.00000 ; dih
27 30 33 36 3 2.92880 -1.46440 0.20920 -1.67360 0.00000 ; dih
30 33 36 38 3 0.52719 -6.39734 -1.69452 7.56467 0.00000 ; dih
33 36 38 40 3 58.57600 0.00000 -58.57600 0.00000 0.00000 ; dih
36 38 40 42 3 0.52719 -6.39734 -1.69452 7.56467 0.00000 ; dih
38 40 42 43 3 0.76567 2.29701 0.00000 -3.06269 0.00000 ; dih
38 40 46 47 3 0.76567 2.29701 0.00000 -3.06269 0.00000 ; dih

[ dihedrals ]
; ai aj ak al funct cp mult imp
; 1 3 9 2 1 180.000 4.602 2 ; imp
3 1 4 17 1 180.000 4.602 2 ; imp
4 3 6 5 1 180.000 4.602 2 ; imp
6 4 8 7 1 180.000 4.602 2 ; imp
8 6 9 15 1 180.000 4.602 2 ; imp
9 1 8 10 1 180.000 4.602 2 ; imp
22 20 23 26 1 180.000 43.932 2 ; imp
36 33 38 37 1 180.000 62.760 2 ; imp
38 36 39 40 1 180.000 62.760 2 ; imp

[ dihedrals ]
; ai aj ak al funct cp mult imp
; 1 3 9 2 1 180.000 4.602 2 ; imp
3 1 4 17 1 180.000 4.602 2 ; imp
4 3 6 5 1 180.000 4.602 2 ; imp
6 4 8 7 1 180.000 4.602 2 ; imp
8 6 9 15 1 180.000 4.602 2 ; imp
9 1 8 10 1 180.000 4.602 2 ; imp
22 20 23 26 1 180.000 43.932 2 ; imp
36 33 38 37 1 180.000 62.760 2 ; imp
38 36 39 40 1 180.000 62.760 2 ; imp

```